Proceedings of the DIS'2004, Štrbské Pleso, Slovakia

STUDIES OF FORWARD JETS IN DIS

ALBERT KNUTSSON *
Lund University, Sweden
Box 118, 222 22 Lund, Sweden
E-mail: albert.knutsson@hep.lu.se

Results are presented on forward jet measurements in deep inelastic electron-proton scattering from the H1- and ZEUS-experiments. The analysis goal is to target new parton dynamics. The results from the H1-experiment include an inclusive cross-section measurement as a function of x_{Bj}, a triple differential cross-section as a function of x_{Bj} in bins of Q^2 and the forward jet transverse momentum, p_t^2, and a cross-section for topologies with two central and one forward jet. From ZEUS inclusive cross-sections as a function of x_{Bj}, Q^2, p_t and η_{jet} are presented. The measured cross-sections are compared to NLO (α_s^2) calculations and to predictions from several QCD Monte Carlo models.

1 Introduction

The kinematic range at HERA covers values of the Bjorken scaling variable, x_{Bj}, as small as $\sim 10^{-4}$ at Q^2 of a few GeV. This is a region where pertubative calculations are still expected to be valid, and where $F_2(x, Q^2)$ rises strongly with decreasing x_{Bj}. This rise is well described by NLO DGLAP [1] evolution. However, studies of final states like di-jet production or energy flow measurement show that low order DGLAP dynamics are not sufficient to describe the data. In order to search for alternative parton dynamics, resulting in non-ordering in virtuality (BFKL [4]), measurements of jets produced close to the proton direction (forward jets) offer good opportunities. By applying requirements on Q^2, the transverse momentum and the fractional proton momentum carried by the forward jet, it is possible to control the kinematics of the parton evolution.

The DGLAP scheme resums terms in $\log(Q^2)$ in the pertubative expansion of α_s, resulting in emissions ordered in parton virtuality. Since terms in $\log(1/x)$ are neglected, DGLAP is not expected to describe the data for very small x-values. These terms are resummed in the BFKL scheme, giving strong ordering in the fractional momentum of the propagating partons, x. The CCFM [5] scheme is often seen as a unification of DGLAP and BFKL, since it resums terms of both types, $\log(Q^2)$ and $\log(1/x)$. CCFM accounts for colour coherence effects by requiring angular ordering of the emissions.

Data collected in 1997 and 1996/97 have been used for the H1 and ZEUS measurements, respectively.

*On behalf of the H1 and ZEUS collaborations

2 Monte Carlo models and QCD calculations

The NLO di-jet calculations were performed using the DISENT [3] program with the CTEQ6M parametrization of the proton parton density. The average p_t^2 of the forward jets in all selected events (45 and 67 GeV^2 for the inclusive and triple differential cross-section measurements, respectively) was used for the renormalization scale, μ_r^2, by the H1 collaboration, whereas the ZEUS collaboration used $\mu_r^2 = Q^2$. The renormalization scale uncertainty was estimated by varying the scale, μ_r^2, by a factor of four.

The data are also compared to cross-sections predicted by the Monte Carlo generators RAPGAP [6] (RG), LEPTO [7], ARIADNE [9] and CASCADE [10]. RAPGAP and LEPTO (MEPS) use LO matrix elements (ME) with DGLAP parton showers (PS). RAPGAP offers the possibility to add contributions from resolved virtual photon processes, where an additonal DGLAP parton ladder is generated between the hard subsystem and the photon. In the following RAPGAP DIR represents direct interactions, whereas RAPGAP DIR+RES(=TOT) denotes processes including resolved photons. ARIADNE is based on the Colour-Dipole-Model [2] (CDM), in which colour dipoles produce radiation non-ordered in virtuality. Also in these cases the CTEQ6M parametrization of the parton density has been used. CASCADE implements the CCFM formalism, which also gives non-ordering in virtuality, and uses the so-called J2003-set-2 version of the unintegrated gluon density. That means that both singular and non-singular terms are included in the splitting function.

3 Event and Jet Selection

The ZEUS collaboration measures the forward jet cross-sections from a sample of events obtained by applying the cuts $E'_e > 10$ GeV, $y > 0.04$ and $Q^2 > 25$ GeV^2. Jets are selected within two different pseudorapidity ranges in the forward region, (2) $0 < \eta_{jet} < 3$, and are required to have a transverse momentum $p_t > 6$ GeV. The phase space for DGLAP evolution is suppressed by requiring similar virtualities at the two end points of the parton ladder, which is achieved by selecting forward jets with $0.5 < p_t^2/Q^2 < 2$. To further suppress inclusive DIS events a restriction is imposed on the hadronic angle, $\cos\theta_\gamma < 0$, such that QPM jet events are suppressed.

In order to obtain a clean DIS sample the H1 experiment applies the cuts $E'_e >$ 10 GeV, $156^o < \theta_e < 175^o$, $0.1 < y < 0.7$, $0.0001 < x_{Bj} < 0.004$, 5 GeV$^2 < Q^2 <$ 85 GeV^2. The selected jets are here forced to be as close as possible (limited by detector effects) to the proton remnant by the requirement $1.735 < \eta_{jet} < 2.79$, and to have a transverse momentum $p_t > 3.5$ GeV. The DGLAP phase space is suppressed by the cut $0.5 < p_t^2/Q^2 < 5$. To further favour BFKL dynamics, i.e. ordering in x, the fractional momentum of the proton carried by the forward jet, x_{jet}, is required to be much larger than x_{Bj} via the cut $x_{jet} > 0.035$. If more than one jet fullfills these criteria, which happens in $\sim$1/100 of all selected events, the most forward going jet is selected as the forward jet. In all cases the jets are reconstructed by the inclusive k_t-algorithm.

By selecting two hard jets in addition to the forward jet, an alternative method to target BFKL dynamics is tried (H1). All three jets are required to have $p_t > 6$ GeV, such that DGLAP dynamics are not favoured. In this method the p_t^2/Q^2-cut is avoided. The rapidities of the jets are defined as to be $\eta_{JET1} < \eta_{JET2} < \eta_{FWDJET}$. The 2+forward jet cross-section is measured separately for $\Delta\eta_1 = \eta_{JET1} - \eta_{JET2} < 1$ and $\Delta\eta_1 > 1$ as a function $\Delta\eta_2 = \eta_{JET2} - \eta_{FWDJET}$. By requiring $\Delta\eta_1 < 1$ the invariant mass of the di-jet system is forced to be small, and thus it also takes a small x_{gluon} to create this system. This means that there is a room for a larger number of splittings in the parton ladder, i.e. a larger amount of emissions is possible and thus a BFKL-like evolution in x is favoured. If instead $\Delta\eta_1 > 1$ the invariant di-jet mass is larger and the parton ladder shorter since a larger propagator momentum has been used to create the di-jet system.

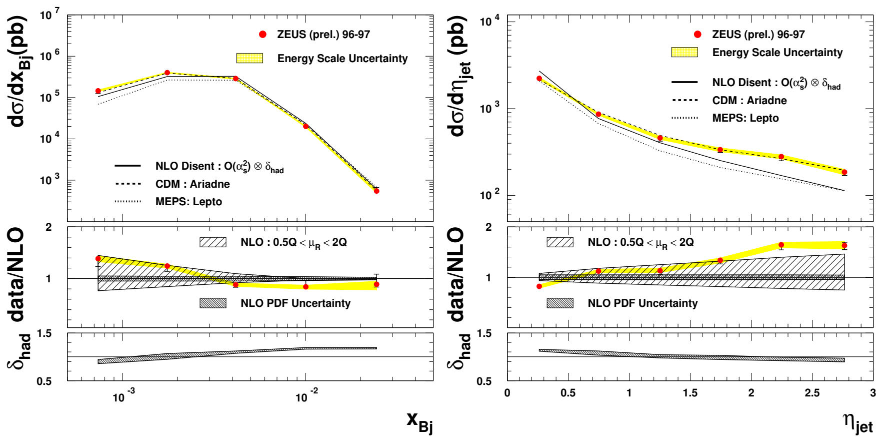

Figure 1. Inclusive event and jet cross-sections from ZEUS for $0 < \eta_{jet} < 3$ compared to an NLO calculation and QCD Monte Carlo models.

4 Forward Jet cross-sections

The ZEUS measurements of inclusive forward jet production are shown in Fig. 1 and Fig. 2 for the two different pseudorapidity regions. The cross section as a function of x_{Bj} in the wider pseudorapidity range, shown in Fig. 1 (left hand plot), is fairly well described by both the NLO calculations and the models. However, the ME+DGLAP PS (LEPTO) model and the NLO calculations deviate from the data at small x_{Bj}. The disagreement of the NLO prediction is, however, well inside the renormalization scale uncertainty. Looking at the pseudorapidity distribution (right) it is noticed that in the more forward region the sensitivity to higher order emissions is higher, but the scale uncertainty is on the other hand larger. In order to study the region with the largest discrepancy with NLO the cross-sections were measured for $2 < \eta_{jet} < 3$, Fig. 2. Here the NLO scale uncertainty increases and the prediction diverges from the data again as x_{Bj} decreases. The scale uncertainty is increased compared to the wider pseudorapidity selection. NLO and ME+DGLAP PS fail for both smaller Q^2 and smaller E_T, which are related by the p_t^2/Q^2-cut. In all cases CDM describes the cross-sections very well.

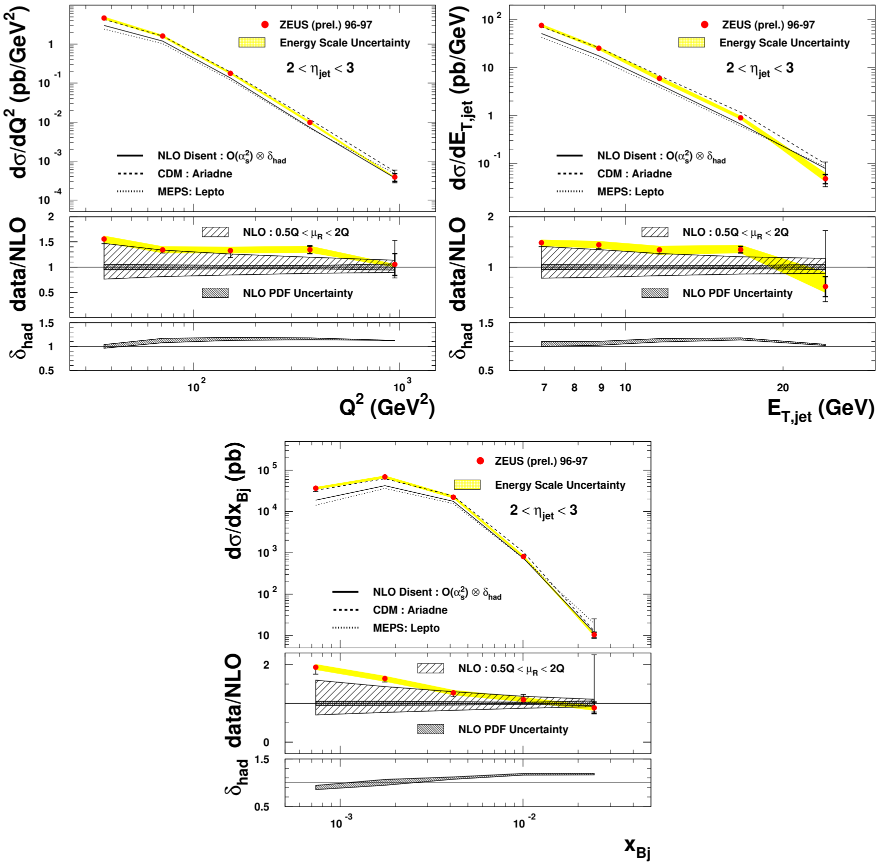

Figure 2. Inclusive event and jet cross-sections from ZEUS for $2 < \eta_{jet} < 3$ compared to an NLO calculation and QCD Monte Carlo models.

In Fig. 3 the H1 inclusive forward jet cross-section as a function of x_{Bj} is compared to an NLO di-jet calculation (left) and QCD model predictions (right). Similar to the cross-sections measured by ZEUS, both NLO calculations and ME+DGLAP PS (RAPGAP DIR) fail in describing the H1 data for low x_{Bj}. In this case the NLO renormalization scale uncertainty does not account for the observed deviation. It should be noted that different renormalization scales have been used by H1 and ZEUS. By adding the contribution from resolved photons, RAPGAP DIR+RES, the predicted cross-section significantly increases and the data are described over the full x_{Bj} range except for the lowest x_{Bj}-bin. The CCFM model (CASCADE) has some problems in describing the shape of the cross-section. CDM is in better agreement with data than CASCADE but predicts too low a cross-section at small x_{Bj}. One reason for the higher sensitivity to higher order emissions for small x_{Bj} is the x_{JET}-cut, which increases the range in longitudinal momentum fraction as x_{Bj} decreases, and thus opens up the phase space for higher order emissions.

For the triple differential cross-section (H1) the p_t^2/Q^2-restriction is replaced

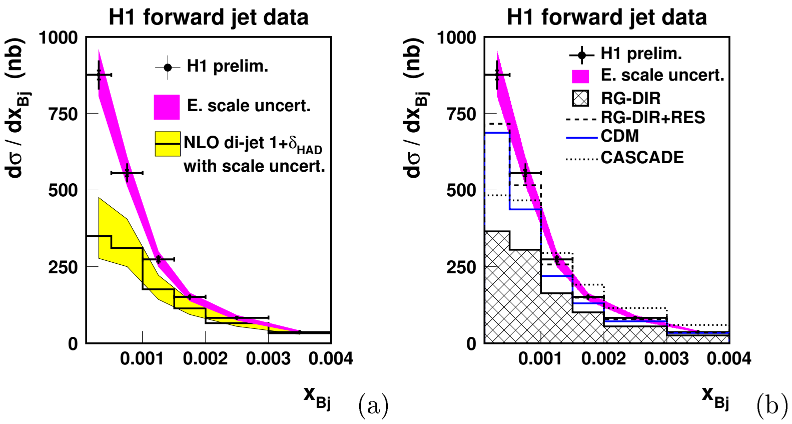

Figure 3. Inclusive forward jet cross-section as a function of x_{Bj} compared to NLO di-jet calculations (a) and to QCD Monte Carlo models.

by a binning in p_t^2 and Q^2 giving the possibility to separate the phase space into different kinematic regions in $p_t^2/Q^2 = r$. For $p_t^2 < Q^2$ the emissions can be ordered in virtuality, i.e. the region in phase space where normal DGLAP dynamics are most likely to be applicable. The region with $p_t^2 \sim Q^2$ is the region where DGLAP dynamics are supressed, and thus the region where BFKL dynamics are expected to be most favoured. Finally for $p_t^2 > Q^2$ the components of the virtual photon can be resolved. Comparing the data to the NLO calculations, Fig. 4 (upper), we again see that for low x_{Bj} and low Q^2 the data exceed the predictions by NLO calculations, whereas for high x_{Bj} the data are described by NLO calculations.

In Fig. 4 (lower) the same data are compared to different QCD models. MEPS fails in the full phase space but is significantly closer to the data in the DGLAP-like region, which however is not a clean DGLAP region, since r is not $\ll 1$. This could explain why RG-DIR does not describe the data at small x_{Bj}. The resolved photon contribution (RG-TOT) in this region is too large, but CDM describes the data within the uncertainties. In the BFKL-like region the DGLAP PS with a resolved photon component describes the data, which also is the case in the resolved photon-like region, where CDM overshoots the data significantly in some bins. CCFM shows the same behavour as for the inclusive cross-section, where too high a cross-section is predicted for high x_{Bj} and too low a cross-section for low x_{Bj}.

Fig. 5 shows the 2+forward jet cross-sections as function of $\Delta\eta_2$ for $\Delta\eta_1 < 1$ and $\Delta\eta_1 > 1$. For $\Delta\eta_1 > 1$, where BFKL dynamics are expected to be supressed, CASCADE is only close to describing the data in the two highest $\Delta\eta_2$-bins. On the other hand for $\Delta\eta_1 < 1$ CASCADE is in agreement with the data in these two bins indicating that this region, as expected, is governed by dynamics different from where $\Delta\eta_1 > 1$. CDM gives the overall best description of data.

5 Summary/Conclusions

It has been shown that NLO calculations and ME+DGLAP PS are unable to describe the HERA jet data at small x_{Bj}. The deviation of the NLO calculations

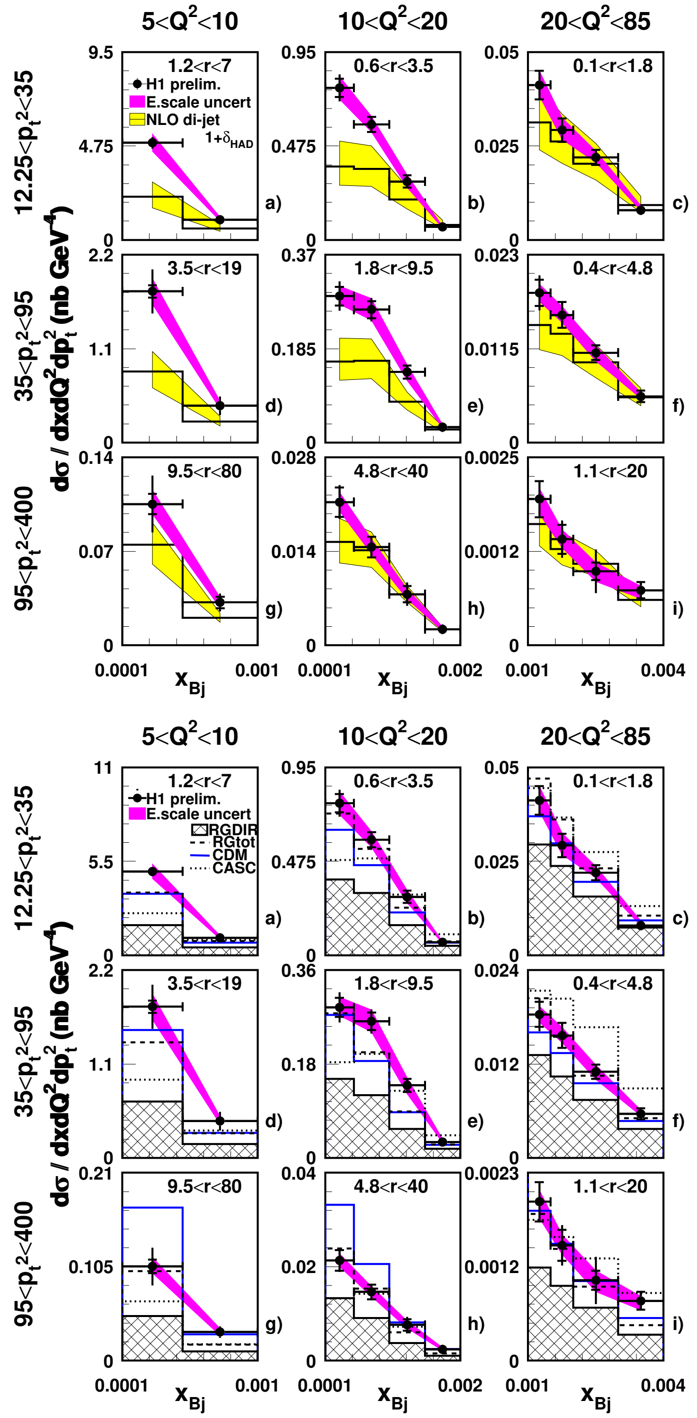

Figure 4. Triple differential forward jet cross-section as a function of x_{Bj} in bins of Q^2 and $p_{\mathrm{t,\ jet}}$ compared to NLO di-jet calculations (DISENT) (upper) and QCD models (lower). In each plot the possible values of $p_t^2/Q^2 = r$ is written.

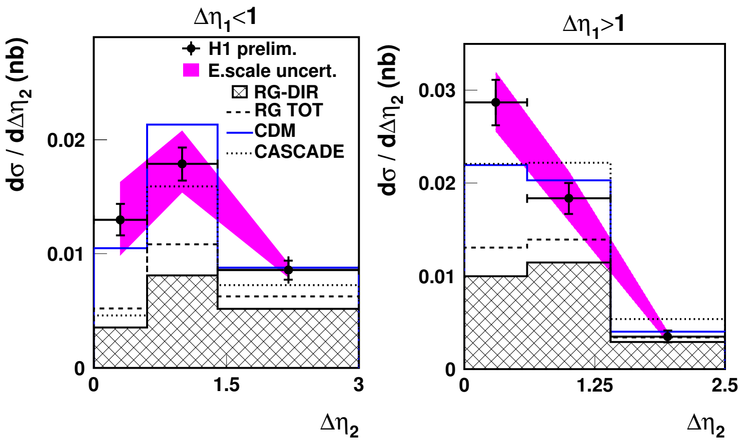

Figure 5. 2+forward jet cross-section as a function of the pseudorapidity separation between the most forward of the di-jets and the forward jet compared to QCD Monte Carlo models.

suggests that higher order terms are important. Comparing data and QCD models shows that models breaking the strong ordering in virtuality (CDM, RAPGAP DIR+RES, CASCADE) give better agreement with data than NLO calculations and standard ME+DGLAP PS. The two statements above are mostly valid for the forward region, where the sensitivity to higher order emissisions is largest. A 2+forward jet cross-section has been measured as an alternative approach to target non-DGLAP-like dynamics. Here only CDM and to a somewhat lesser extent CASCADE describe the data, while RAPGAP with the resolved photon contribution is significantly below the data.

References

1. V. Gribov and L. Lipatov, Sov. J. Nucl. Phys. **15** (1972) 438 and 675
   L. Lipatov, Sov. J. Nucl. Phys. **20** (1975) 94
   G. Altarelli and G. Parisi, Nucl. Phys. **B 126** (1977) 298
   Y. Dokshitzer, Sov. Phys. JETP **46** (1977) 641
2. G. Gustafson, U. Pettersson Nucl. Phys. **C 306** (1988) 746
3. S. Catani *et al.*, Phys. Lett.**B 378** (1996) 287,*Nucl.Phys.***B 485** (1997) 291
4. E. Kuraev, L. Lipatov and V. Fadin, Sov. Phys. JETP **45** (1977) 199
   Y. Balinsky and L. Lipatov, Sov. J. Nucl. Phys. **28** (1978) 822
5. M. Ciafaloni, Nucl. Phys. **B 296** (1988) 49
   S. Catani, F. Fiorani and G. Marchesini, Phys. Lett. **B 234** (1990) 339
   G. Marchesini, Nucl. Phys. **B 445** (1995) 49
6. H. Jung, https://www.desy.de/ jung/rapgap.html
7. G. Ingelman *et al.*, http://www3.tsl.uu.se/thep/lepto/
8. A. Kwiatkowski *et al.*, Comp. Phys. Comm. **69** (1992) 155
9. L. Lönnblad, Z. Pys. **C 65** (1995) 285
10. H. Jung, Comp. Phys. Comm. **143** (2002) 100